Chiral Metal-Dithiolene/Viologen Ion Pairs: Synthesis and Electrical Conductivity**

Horst Kisch,*[a] Bernhard Eisen,[a] Robert Dinnebier,[b] Kenneth Shankland,[c] William I. F. David,[c] and Falk Knoch[a]

Dedicated Professor Dieter Sellmann on the occasion of his 60th birthday

Abstract: Enantiomerically pure dithiolene complexes $NBu_4[Ni\{(R,R)\text{-diotte}\}_2]$ and $NBu_4[Ni\{(S,S)\text{-diotte}\}_2]$ ($diotte^{2-}$ = a 1,3-dioxolane-tetrathiaethylene), were prepared from the corresponding enantiomers of a $diotte^{2-}$ precursor. The structure of the precursor was solved by single-crystal X-ray analysis; desulfurization afforded a novel tetrathiafulvalene derivative. Combination of the complex monoanion with the enantiomers of the viologen derivative bis(2-methyl-3-hydroxypropyl)-4,4′-dipyridinium ($HiBV^{2+}$) afforded enantiomeric and diastereomeric ion–pair complexes of the type $HiBV[Ni(diotte)_2]_2$. For comparison, the analogous compounds $A[Ni(diotte)_2]_2$, (A^{2+} = methyl (MV^{2+}), octyl (OV^{2+}), stearyl (StV^{2+}) viologen or two 2,2′-bipyridinium acceptors), HiBV-[Ni(diotte)L] {L = mnt^{2-} (maleonitrile-1,2-dithiolate), $dmit^{2-}$ (2-thioxo-1,3-dithiol-4,5-dithiolate)}, $MV[Ni(dmit)_2)]_2$, $[Ni(diotte)_2]$, and [Ni(diotte)(dmit)] were synthesized. An X-ray powder diffraction structural analysis of MV-$[Ni(dmit)_2)]_2$ revealed the presence of mixed stacks that contain the sequence anion–anion–cation. While no short contacts are observable within a stack, these are observed between the stacks for the dication–anion interaction by short S···H distances in the range of 2.77 to 2.86 Å, and for the anion–anion interaction short S···S distances of 3.55 to 3.65 Å. In agreement with the absence of intrastack interactions, no ion–pair charge-transfer band can be detected in this and the other complexes. ESR and UV/Vis data suggest that in $[Ni(diotte)_2]^-$ electron delocalization is less pronounced than in the corresponding mnt^{2-} and $dmit^{2-}$ complexes. The specific electrical conductivity (σ) of pressed powder pellets ranges from 10^{-2} to $10^{-12}\ \Omega^{-1}cm^{-1}$ and in all cases increases with increasing temperature (293–393 K) according to an Arrhenius law. Corresponding activation energies vary from 0.14 to 0.93 eV and increase linearly with $\log\sigma$ for structurally similar ion pairs. Charge generation is postulated to occur by disproportionation of the monoanion as suggested by the almost linear increase of $\log\sigma$ with decreasing disproportionation energy. The conductivity of diastereomers of ions with two unlike configurations like [(*S*,*S*)-HiBV]-$[Ni\{(R,R)\text{-diotte}\}_2]_2$ ($1.1\times10^{-11}\ \Omega^{-1}cm^{-1}$) is one to two orders of magnitude higher as compared to the diastereomers with two like-configured ions.

Keywords: chirality · cyclic voltammetry · dithiolenes · enantiomers · nickel · viologens

Introduction

The molecular design of a solid-state property is a central topic of materials science. Recently we have reported that ion–pair charge-transfer (IPCT) complexes of the type $A^{2+}[ML_2]^{2-}$ that consist of a planar dianionic dithiolene metalate $[ML_2]^{2-}$ (M = Ni, Pd, Pt; L = a 1,2-ethenedithiolate) and a pseudo-planar dicationic 4,4′- and 2,2′-bipyridinium derivative (A^{2+}) are molecular semiconductors.[2] As pressed powder pellets they exhibited specific electrical conductivities in the range of 10^{-10} to $10^{-3}\ \Omega^{-1}cm^{-1}$. The presence of an IPCT band in the diffuse reflectance spectra of these ion pairs indicated a supramolecular electronic interaction between the components. Although in the ground state only about 0.01 % of an electron is transferred from the dianion to the dication, modulation of this very weak effect by proper selection of the components redox potentials allows a quantitative tuning of the conductivity. This correlation holds only as long as the geometry of the acceptor ions does not deviate too far from planarity. In this case, as indicated by the X-ray structural analyses of various $A^{2+}[M(mnt)_2]^{2-}$ (M = Ni, Pd, Pt; mnt = maleonitrile-1,2-dithiolate) complexes[2b] and of

[a] Prof. Dr. H. Kisch, Dr. B. Eisen, Dr. F. Knoch
Institut für Anorganische Chemie, Universität Erlangen-Nürnberg
Egerlandstrasse 1, 91058 Erlangen (Germany)
Fax: (+49) 9131-8527363
E-mail: kisch@anorganik.chemie.uni-erlangen.de

[b] Dr. R. Dinnebier
Lehrstuhl für Kristallographie der Universität Bayreuth
Universitätsstrasse 30, 95447 Bayreuth (Germany)

[c] Dr. K. Shankland, Dr. W. I. F. David
ISIS Facility, Rutherford Appleton Laboratory
Chilton, Didcot, Oxford, OX11 0QX (UK)

[**] Charge-Transfer Complexes of Metal Dithiolenes, Part XXVII. For Part XXVI see ref. [1].

0947-6539/01/0703-0738 $ 17.50+.50/0

$DPD^{2+}[Ni(dmit)_2]^{2-}$ (DPD^{2+} = *trans*-4,4′-azobis(1-methylpyridinium), dmit = 2-thioxo-1,3-dithiol-4,5-dithiolate)[1] mixed donor–acceptor stacks are formed in the solid state. For a corresponding series of complexes, which contain mainly the dmit ligand, the logarithm of the specific electrical conductivity increased linearly over seven orders of magnitude when the driving force (ΔG_{12}) of electron transfer from the dianion to the dication was varied from 0.7 to −0.1 eV through modification of the bipyridinium acceptor. This suggested that charge generation occurred by electron transfer from the dianion to the dication and, therefore, the activation energy of this process may determine the conductivity. Accordingly, the free activation enthalpy, as calculated within the Hush–Marcus model from the driving force and the energy of IPCT transition, also correlated with conductivity. From these results we assumed that the reason for this unique relation between driving force and conductivity is the presence of the weak IPCT interaction. To test this hypothesis, 1:2 ion–pair complexes of the type $A^{2+}[ML_2]_2^{2-}$ were prepared that do not exhibit IPCT bands. Furthermore, the absence of a charge-transfer interaction opens the possibility to study the influence of diastereoisomerism on electrical properties when chiral ions are present. Accordingly, chiral viologens and chiral anionic metal–dithiolenes were combined to form diastereomeric and enantiomeric ion–pair complexes, and their electrical conductivities were measured. Although a few chiral bipyridinium derivatives have already been reported,[3] we are not aware of the synthesis of enantiomeric metal–dithiolene complexes. Furthermore, the literature on the relationship between stereoisomerism and electrical properties is very scarce. Rare examples are two structurally different radical-cation salts of tetrathiafulvalene, both obtained only as one unique enantiomer.[4, 5] In contrast to this, the ion–pair complexes reported in the following are available as both enantiomers and corresponding diastereomers.

Abstract in German: *Enantiomerenreine Dithiolenkomplexe des Typs $NBu_4[Ni(R,R\text{-diotte})_2]$ und $NBu_4[Ni(S,S\text{-diotte})_2]$, $diotte^{2-}$ = ein 1,3-Dioxolan-Tetrathiaethylenligand, wurden ausgehend von den beiden Enantiomeren eines $diotte^{2-}$-Vorläufers dargestellt. Die Desulfurierung des Vorläufers führte zu einem neuen Tetrathiafulvalenderivat. Metathetische Umsetzung der Tetrabutylammoniumkomplexe mit den optischen Antipoden des Viologenderivats Bis(2-methyl-3-hydroxypropyl)-4,4′-dipyridinium ergab enantiomere und diastereomere Ionenpaarkomplexe des Typs $HiBV[Ni(diotte)_2]_2$. Zum Vergleich wurden auch die analogen Komplexe $A[Ni(diotte)_2]_2$, A^{2+} = Methylviologen (MV^{2+}), Octyl- und Stearylviologen oder zwei 2,2′-Bipyridiniumderivate, $HiBV[Ni(diotte)L]$, $L = mnt^{2-}$ (Maleonitril-1,2-dithiolat), $dmit^{2-}$ (2-Thioxo-1,3-dithiol-4,5-dithiolat), $MV[Ni(dmit)_2)]_2$, $Ni(diotte)_2$ und $Ni(diotte)(dmit)$ synthetisiert. Hochaufgelöste Pulverdiffraktometrie zeigt, daß die Festkörperstruktur von $MV[Ni(dmit)_2]_2$ aus gemischten Stapeln der Reihenfolge Anion–Anion–Kation besteht. Während innerhalb eines Stapels keine kurzen Kontakte auftreten, wird eine Wechselwirkung zwischen den Stapeln durch kurze S···H–Abstände von 2.77 bis 2.86 Å zwischen Dikation und Anion und kurze S···S–Abstände von 3.55 bis 3.65 Å zwischen zwei Anionen angedeutet. In Einklang mit dem Fehlen von intrakolumnaren Dikation–Anion-Wechselwirkungen besitzen die Komplexe keine Ionenpaar–Charge-Transferbande. ESR- und UV/Vis-Spektren deuten darauf hin, daß die Elektronendelokalisierung in $[Ni(diotte)_2]^-$ weniger stark ausgeprägt ist als in $[Ni(mnt)_2]^{2-}$ und $[Ni(dmit)_2]^{2-}$. Die spezifische elektrische Leitfähigkeit (σ) von Pulverpresslingen liegt im Bereich von 10^{-2} bis $10^{-12}\ \Omega^{-1}cm^{-1}$ und steigt für alle Komplexe mit steigender Temperatur (293–393 K) gemäß einem Arrhenius-Gesetz. Die Aktivierungsenergien variieren von 0.14 bis 0.93 eV und steigen linear mit log (σ) für strukturell ähnliche Ionenpaare. Es wird vorgeschlagen, daß die Ladungsträgererzeugung durch eine Disproportionierung zustande kommt, da log (σ) etwa linear mit der Disproportionierungsenergie des Monoanions zunimmt. Die Leitfähigkeit von Diastereomeren mit Ionen ungleicher Konfiguration wie $(S,S)\text{-}HiBV[Ni(R,R\text{-diotte})_2]_2$ ($1.1 \times 10^{-11}\ \Omega^{-1}cm^{-1}$) ist um ein bis zwei Größenordnungen höher als im Falle zweier gleich konfigurierter Ionen.*

Results and Discussion

Syntheses: To introduce chirality in the planar dithiolene metalates an asymmetric ethenedithiolate ligand was synthesized. By analogy of the synthesis of diop (diop = (*4S,5S*)-4,5-bis-(diphenylphosphinomethyl)-2,2-dimethyl-1,3-dioxolane) the precursors **1**, **2** (see Figure 1) and their enantiomers (*S,S*)-**2**

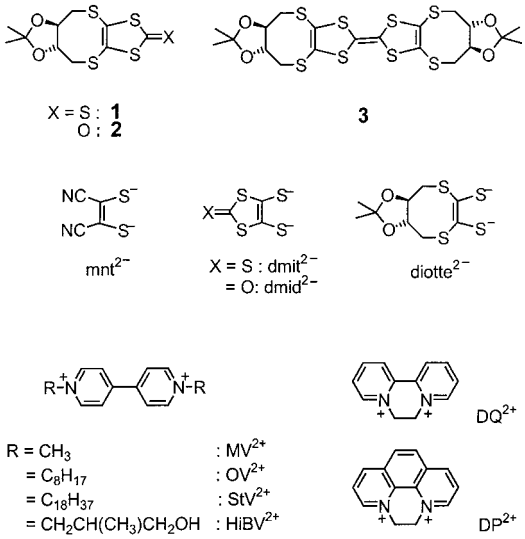

Figure 1. Structures of the ligands referred to in this paper.

and (*R,R*)-**2** were prepared by the alkylation of $(NBu_4)_2[Zn(dmit)_2]$[6] and $(NBu_4)_2[Zn(dmid)_2]$ (dmid = 2-oxo-1,3-dithiol-4,5-dithiolate),[7] respectively, with the racemate and enantiomers of 4,5-bis(bromomethyl)-2,2-dimethyl-1,3-dioxolane[8] in dry DMF at 135 °C. In contrast, to similar alkylations with uncomplexed ethenedithiolate generated in situ,[6, 9] this method has less side reactions, the produced Zn^{2+} and NBu_4^+ salts can be easily separated, and it is not necessary to work under inert gas atmosphere. Isolated yields were in the range of 60–75%. IR reaction spectroscopy[10] indicated that in

DMF (at 135 °C) complete transformation occurred already after 6 h, but the reaction time was 48 h in *n*BuOH (117 °C). When the diop—precursor 4,5-bis(tosyloxymethyl)-2,2-dimethyl-1,3-dioxolane[11]—was used as alkylation agent, the amount of product was too small for preparative isolation; it is known that tosylates are poorer leaving groups than bromides in nucleophilic substitutions by dithiolates.[12] In addition to this direct synthesis of **2** from $(NBu_4)_2[Zn(dmid)_2]$, compound **2** was also prepared by desulfurization of **1** with mercuric acetate.[13] When the latter was replaced by triethylphosphite the tetrathiafulvalene derivative **3** (Figure 1) was obtained in 68% yield. This is a well-known reaction[14] in which the oxygen analogues in general afford higher yields than the sulfur compounds;[15] accordingly, compound **2** and not **1** was used as starting material. Cyclic voltammetry of **3** revealed the presence of two reversible peaks at +0.60 and +1.01 V, (CH_2Cl_2 vs SCE). Similar redox potentials were reported for tetrathiafulvalene derivatives containing a cyclooctene ring.[16]

The structure of (*R*,*R*)-**2** was solved by single-crystal X-ray structural analysis. The dmid fragment retains its planarity, while the remaining dioxolane part is arranged almost perpendicular to this plane as indicated by the C2-S3-C4 and C3-S4-C7 angles of 100.5(3) and 101.1(3)°, respectively (Table 1, Figure 2). The central dithiacyclooctene ring adopts a half-chair conformation. Within the dmid skeleton the average C–S bond length of 1.75 Å is 0.07 Å shorter than the C4–S3 and C7–S4 bonds; this suggests some double-bond character. The expected *R*,*R* configuration follows from the stereochemistry at C5 and C6. The integrated peak areas of the CD spectra of (*R*,*R*)-**2** and its enantiomer (*S*,*S*)-**2** are in excellent agreement; this suggests enantiomeric purity (Figure 3a top).

In agreement with the literature[6, 17, 18] no ν(C=C) bands are observable in the IR spectra of **1**–**3**. For **1** two ν(C=S) absorptions are found at 1065 and 1045 cm^{-1}, while the intense ν(C=O) band of **2** appears at 1658 cm^{-1}. For the ring-opened salt K_2[diotte] (diotte^{2-} = dioxolane-tetrathiaethylene ligand; Figure 1), a ν(C=C) absorption is detected at 1663 cm^{-1}, which compares well with the value of 1665 cm^{-1} reported for K_2[dddt] (dddt^{2-} = 5,6-dihydro-1,4-dithiin-2,3-dithiolate).[19a] According to published procedures for the basic hydrolysis of isodithione ($C_3H_2OS_2$) related ring systems,[10, 19] the reaction between **2** and KOEt was not performed in EtOH[20] but in THF as solvent; this resulted in a much higher yield. The thus obtained powder of K_2[diotte] slowly decomposed even under an argon atmosphere, while it was more stable in alcoholic solution.

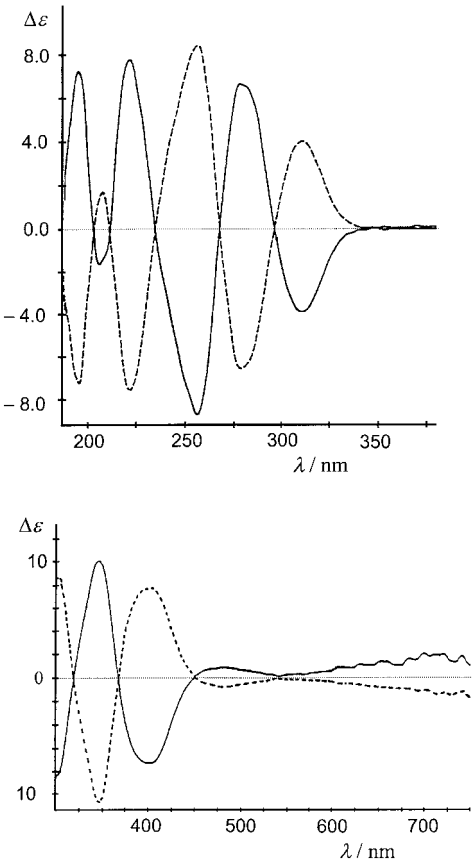

Figure 3. CD spectra of (*R*,*R*)-**2** (——, $c = 0.555 \times 10^{-3}$ M) and (*S*,*S*)-**2** (– – –, $c = 0.529 \times 10^{-3}$ M) in CH_2Cl_2 (top) NBu_4[Ni{(*R*,*R*)-diotte}$_2$] (——, $c = 0.151 \times 10^{-3}$ M) and NBu_4[Ni{(*S*,*S*)-diotte}$_2$] (– – –, $c = 0.169 \times 10^{-3}$ M) in MeCN (bottom).

Table 1. Selected bond lengths [Å] and angles [°].[a]

2						MV[Ni(dmit)$_2$]$_2$	
C1–O1	1.205(9)	S1-C1-S2	112.4(4)	Ni–S7	2.190(3)	S7-Ni-S6	92.000(9)
C1–S2	1.765(8)	C1-S2-C3	96.7(3)	Ni–S6	2.190(3)	Ni-S7-C5	101.000(8)
C2–C3	1.340(9)	S2-C3-C2	116.8(5)	S7–C5	1.682(3)	Ni-S6-C4	101.000(10)
C2–S3	1.755(6)	C2-C3-S4	125.0(5)	C5–C4	1.319(7)	S7-C5-c4	123.000(11)
C3–S4	1.738(6)	C3-S4-C7	101.3(3)	C4–S6	1.682(3)	S6-C4-C5	123.000(13)
S2–C3	1.747(6)	S4-C7-C6	116.1(4)	C4–S9	2.525(4)	Ni-S6-C4	101.000(10)
S3–C4	1.819(6)	O1-C1-S2	124.0(6)	C5–S9	1.682(3)	S9-C6-S10	123.92(9)
S4–C7	1.817(6)	C5-C6-C7	116.4(5)	C6–S9	1.619(2)	S8-C6-S10	123.93(9)
C6–C7	1.502(8)	S2-C2-S4	118.2(4)	C6–S8	1.619(2)		
O2–C8	1.409(7)	C2-S3-C4	100.5(3)	C6–S10	1.666(3)		

[a] For structural parameters of NBu_4[Ni(dmit)$_2$] and (MV)Cl_2 see refs. [31, 47].

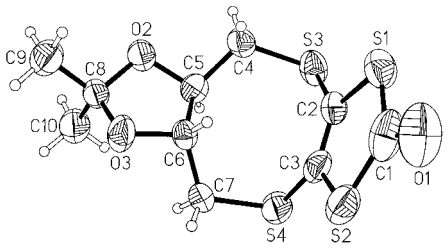

Figure 2. Molecular structure of **2**.

The ^{1}H and ^{13}C NMR spectra of **1**–**3** all are very similar and do not contain any unexpected features (see Experimental Section). Noteworthy is that the signals of C1 and C2,3 are shifted from $\delta = 211$ and 141 in **1** to $\delta = 188$ and 132 in **2**. This upfield shift is in agreement with the lower group electronegativity of a C=O relative to a C=S group.[21] The same chemical shifts as for **2** are observed for the tetrathiafulvalene derivative **3**.

0947-6539/01/0703-0740 $ 17.50+.50/0 *Chem. Eur. J.* **2001**, *7*, No. 3

In the UV/Vis spectrum of **1** the intense π,π* absorption at 367 nm ($\varepsilon = 15\,400\,\text{M}^{-1}\,\text{cm}^{-1}$) exactly fits the value reported for the unsubstituted isotrithione system,[6, 10, 22, 23] while the corresponding thiomethyl-substituted derivative $C_3(MeS)_2S_3$ absorbs at 388 nm owing to extended conjugation. This seems to be prevented in **1** by the unfavorable stereochemistry imposed on S3 and S4 by the dioxolane moiety. No corresponding π,π* absorption band is observed for **2**, which exhibits a broad absorption with a maximum at 267 nm ($\varepsilon = 6000\,\text{M}^{-1}\,\text{cm}^{-1}$) and a shoulder at 310 nm. Two bands are present in the spectrum of **3** at 428 ($\varepsilon = 1600\,\text{M}^{-1}\,\text{cm}^{-1}$) and 323 nm ($\varepsilon = 11\,500\,\text{M}^{-1}\,\text{cm}^{-1}$).

The two enantiomeric viologen derivatives [(*R*,*R*)-HiBV]Br_2 and [(*S*,*S*)-HiBV]Br_2 (Figure 1; HiBV = bis(2-methyl-3-hydroxypropyl)-4,4′-dipyridinium) were isolated in 65 and 50 % yield from the alkylation of 4,4′-dipyridyl with the *R* and *S* enantiomer of 3-bromo-2-methyl-1-propanol in DMF at 135 °C, respectively. In the CD spectrum of [(*R*,*R*)-HiBV]Br_2 in methanol a minimum and maximum of Δε was found at 250 and 290 nm, respectively; the *S*,*S* enantiomer exhibited the mirror image of this spectrum. As expected for a viologen derivative, two reversible waves were observable in the cyclovoltammogram at −0.41 and −0.84 V (acetonitrile vs. SCE).

The monoanionic complex $[Ni(diotte)_2]^-$ was prepared by addition of $NiCl_2 \cdot 6H_2O$ to a solution of $diotte^{2-}$ in methanol. Precipitation of dark-brown $NBu_4[Ni(diotte)_2]$ occurred upon addition of tetrabutylammonium bromide. Yields and purity did not change significantly if $diotte^{2-}$ was added as K_2[diotte] or prepared in situ from **2** and KOEt. After purification by soxhlet extraction and recrystallization, the analytically pure sample was obtained in a yield of 52 %. When the thioderivative **1** was employed instead of **2**, the yield decreased to 13 %. Oxidation of $NBu_4[Ni(diotte)_2]$ with iodine afforded the olive-green neutral complex $[Ni(diotte)_2]$ in 84 % yield. The characteristic dithiolene absorption bands of NBu_4[Ni-(diotte)$_2$] and $[Ni(diotte)_2]$ were observed at 886 ($\varepsilon = 8800$, in CH_2Cl_2) and 823 nm ($\varepsilon = 18\,100\,\text{M}^{-1}\,\text{cm}^{-1}$), respectively. Enantiomeric NBu_4[Ni{(*R*,*R*)-diotte}$_2$] and NBu_4[Ni{(*S*,*S*)-diotte}$_2$] were prepared analogously by using (*R*,*R*)- and (*S*,*S*)-**2**, respectively. Oxidation of these complexes afforded the neutral enantiomers [Ni{(*R*,*R*)-diotte}$_2$] and [Ni{(*S*,*S*)-diotte}$_2$]. Ligand exchange between $[Ni(diotte)_2]$ or its enantiomers and $(NBu_4)_2[NiL_2]$ provided an easy access to the heteroleptic complexes $NBu_4[Ni(diotte)L]$ ($L = dmit^{2-}$, mnt^{2-}) [Eq. (1)], NBu_4[Ni{(*R*,*R*)-diotte}(dmit)], NBu_4-[Ni{(*R*,*R*)-diotte}(mnt)], and NBu_4[Ni{(*S*,*S*)-diotte}(mnt)]. The CD spectra of the last two compounds are shown in Figure 4. Oxidation of $NBu_4[Ni(diotte)(dmit)]$ with iodine afforded the neutral [Ni{(*R*,*R*)-diotte}(dmit)], whereas this was not possible in the case of the less reducing NBu_4-[Ni(diotte)(mnt)].

$$[Ni(diotte)_2] + (NBu_4)_2[NiL_2] \rightarrow 2\,(NBu_4)[Ni(diotte)L] \quad (1)$$

The tetrabutylammonium salts were soluble in DMSO, DMF, THF, and dichloromethane. In the IR spectra (in KBr) the typical metal dithiolene C=C absorptions[24] appeared at 1386 ($NBu_4[Ni(diotte)_2]$), 1379 ($NBu_4[Ni(diotte)(mnt)]$), and

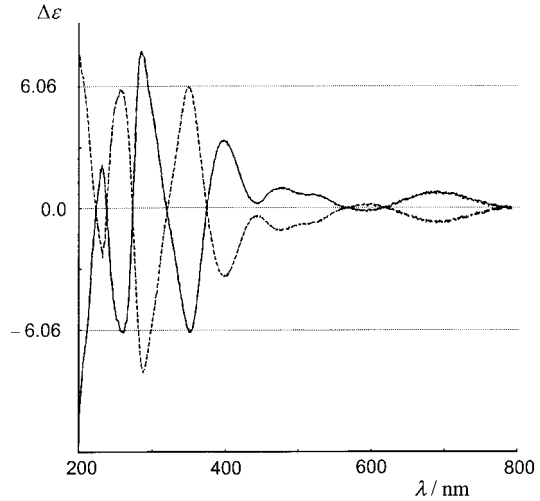

Figure 4. CD spectra of NBu_4[Ni{(*R*,*R*)-diotte}(mnt)] (– – –, $c = 0.092 \times 10^{-3}$ M) and NBu_4[Ni{(*S*,*S*)-diotte}(mnt)] (——, $c = 0.086 \times 10^{-3}$ M) in MeCN.

1368/1350 cm^{-1} ($NBu_4[Ni(diotte)(dmit)]$). The ν(C–S) band at 880 cm^{-1} was not affected. As expected for the neutral compounds, the ν(C=C) vibration was considerably shifted to smaller wavenumbers and appeared for both $[Ni(diotte)_2]$ and [Ni(diotte)(dmit)] at 1270 cm^{-1}; the ν(C–S) vibration of the homoleptic complex was found at the same wavenumber as in $NBu_4[Ni(diotte)_2]$, whereas two bands appeared at 898 and 878 cm^{-1} for the heteroleptic compound.

In the UV/Vis spectrum (CH_2Cl_2) of the neutral complex $[Ni(diotte)_2]$ the π,π* absorption at 823 nm is blue-shifted with respect to $Ni(S_2C_2R_2)_2$, $R = SCH_3$ ($\lambda_{max} = 992$ nm)[25] or R–R = –S-$(CH_2)_2$-S– ($\lambda_{max} = 1049$ nm).[10] As in the case of **2**, this is further evidence for decreased conjugation induced by the $diotte^{2-}$ ligand due to the steric situation at the S3, S4 atoms (vide supra). Accordingly, replacement of one $diotte^{2-}$ ligand by $dmit^{2-}$ increases electron delocalization, and λ_{max} of [Ni(diotte)dmit] is observed at 906 nm. The corresponding monoanions generally absorb at longer wavelengths.[26] As observed for the neutral complexes, the diotte complex $NBu_4[Ni(diotte)_2]$ absorbs at shorter wavelength (875 nm, MeCN) than $[Ni(S_2C_2R_2)_2]^-$, $R = SCH_3$ (1070 nm, DMF)[19d] or R–R = –S-$(CH_2)_2$-S– (1257 nm, DMF).[19d] Since the band positions of $NBu_4[Ni(diotte)_2]$ and $NBu_4[Ni(mnt)_2]$ ($\lambda_{max} =$ 861 nm, MeCN) are similar, the band of the heteroleptic complex $NBu_4[Ni(diotte)mnt]$ is observed at a comparable wavelength of 873 nm (MeCN). In contrast, for NBu_4[Ni-(diotte)dmit] the introduction of the $dmit^{2-}$ ligand shifts this band to 989 nm (MeCN), which corresponds to the arithmetic mean of the absorptions of the two corresponding homoleptic complexes. Both $NBu_4[Ni(diotte)dmit]$ and NBu_4[Ni(diotte)mnt] exhibit only a very weak negative solvatochromic shift of 12 cm^{-1} when acetonitrile is replaced by dichloromethane, in contrast to heteroleptic dithiolene nickelates that contain diimine ligands.[27]

The ESR spectrum of $NBu_4[Ni(diotte)_2]$ exhibited a rhombic *g* tensor with significant deviation from axial symmetry. By analogy with the results from single-crystal measurements of $[Ni(mnt)_2]^-$[28] the *g* values were assigned as

follows; $g_1 \equiv g_{xx}$; $g_2 \equiv g_{yy}$, and $g_3 \equiv g_{zz}$ with g_{xx} and g_{zz} representing the highest and lowest g values (Table 2). From the decreasing g values in the series NBu_4[Ni(diotte)L] (L = diotte^{2-}, mnt^{2-}, dmit^{2-}) one can assume that the electronic delocalization within the {Ni(C_2S_2)$_2$} ring increases in the same direction, as also postulated for similar monoanionic nickel dithiolenes.[19]

Table 2. ESR data for NBu_4[Ni(diotte)L] complexes.

L	$\langle g \rangle$*[a]	$\langle g \rangle$[b]	g_1	g_2	g_3
diotte^{2-}	2.070	2.069	2.156	2.046	2.007
mnt^{2-}	2.065	2.065	2.151	2.044	2.000
dmit^{2-}	2.060	2.062	2.133	2.044	2.033

[a] Calculated from powder spectra; $\langle g \rangle^* = 1/3(g_1 + g_2 + g_3)$; standard deviation of g values is 0.001. [b] From solution spectra obtained in acetone at RT.

Magnetic susceptibility measurements on NBu_4[Ni(diotte)$_2$] afforded a magnetic moment of 1.74 μ_B, which corresponds to the theoretical spin-only value of 1.73 μ_B. For the heteroleptic complexes NBu_4[Ni(diotte)dmit] and NBu_4[Ni(diotte)mnt] the smaller values of 1.37 and 1.59 μ_B, respectively, were obtained. These values are in accordance with the stronger electron-withdrawing properties of the dmit^{2-} and mnt^{2-} ligands with respect that of diotte^{2-} and those also reported for other metal dithiolenes.[29]

The redox potentials support the conclusions drawn from the IR and UV/Vis data on the electronic properties of the new diotte^{2-} ligand. Thus for NBu_4[Ni(diotte)$_2$] in MeCN one irreversible and one reversible wave were observed at $E_1 = +0.42$ V and $E_2 = -0.56$ V (vs SCE), which correspond to oxidation to the neutral and reduction to the dianionic complex, respectively. The E_1 value is more positive than for NBu_4[Ni(dmit)$_2$], $E_1 = +0.18$ V (irreversible), supporting the poorer donor properties of the diotte^{2-} ligand. For the heteroleptic complexes NBu_4[Ni(diotte)dmit] ($E_1 = +0.34$ (irreversible), $E_2 = -0.34$ V) and NBu_4[Ni(diotte)mnt] ($E_1 = +0.74$, $E_2 = -0.20$ V) the measured values are the arithmetic mean of the values for the corresponding homoleptic compounds.

Ion-pair complexes were synthesized in yields of 28–95% by simple metathesis reactions between the corresponding tetrabutylammonium and hexafluorophosphate salts of the dithiolene nickelates and dipyridinium derivatives summarized in Figure 1. The complexes in all cases contain a monoanionic metal dithiolene and a dicationic dipyridinium ion resulting in the 1:2 ion pairs {$A^{2+}[ML_2]_2^{2-}$}. As observed for similar complexes, the IR spectra[30] usually are just a superimposition of the component spectra, except for HiBV[Ni(diotte)(dmit)]$_2$, in which case the ν(OH) band of the dication is shifted by 30–35 cm^{-1} to smaller wavenumbers with respect to that of (HiBV)Br_2. This suggests hydrogen bonding within the ion pair, since the wavenumber of the ν(C=S) vibration is also decreased by 12–13 cm^{-1}.

In contrast to the 1:1 complexes that contain a dianionic metal dithiolene,[2] no IPCT band could be detected for the 1:2 complexes reported herein; this agrees with the absence of short intrastack anion–cation contacts in the model complex MV[Ni(dmit)$_2$]$_2$ (vide infra; MV = metyl viologen). In accordance with previous results,[30] in the diffuse reflectance spectra the characteristic π,π* absorption band at about 900 nm is red-shifted by up to 65 nm relative to that found in solution. The cation exerts only a steric influence as indicated by the weak blue-shift of this band from 916 to 902 and 894 nm and by the stronger red-shift of the absorption onset (Figure 5) from 1340 to 1395 and 1422 nm when methyl viologen

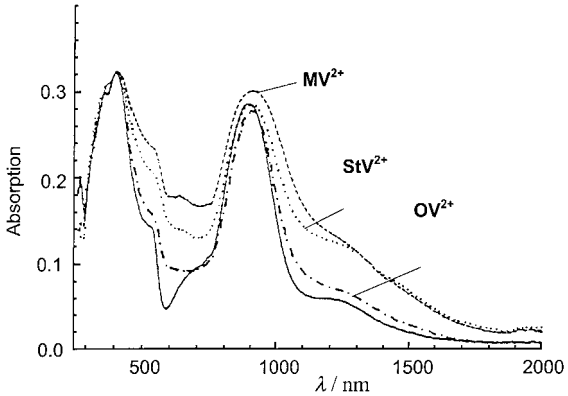

Figure 5. Diffuse reflectance spectra of NBu_4[Ni(diotte)$_2$] (——) and A[Ni(diotte)$_2$]$_2$, A^{2+} = MV^{2+}, OV^{2+}, StV^{2+}.

in MV[Ni(diotte)$_2$]$_2$ is replaced by octyl and stearyl viologen, respectively (Figure 5). In contrast, in the analogous complexes of [Ni(dmit)$_2$]$^-$ E_{on} is blue-shifted when the cation size increases.[30]

Since no crystals big enough for a single-crystal X-ray structural analysis could be obtained for a diotte^{2-} or any other 1:2 complex, MV[Ni(dmit)$_2$]$_2$ was selected for a powder X-ray analysis because in this case the molecular structure of both components is known (see Experimental Section).[2b] The arrangement of the two planar ions is best described as a mixed stack of dication–anion–anion fragments without any evidence for short cation–anion intrastack contacts (Figure 6); all corresponding distances are in the range of 3.65–3.79 Å and therefore significantly larger than 3.33–3.52 Å, the value usually observed in the corresponding charge-transfer complexes of 1:1 stoichiometry. In contrast to [Ni(dmit)$_2$]$^-$ salts with non-redox-active counterions, the monoanion does not form a dimer as indicated by the average interplanar distance of 3.80 Å, which is longer than the 3.44–3.60 Å reported for the dimer.[31–34] Whereas no short intrastack contacts were found, a number of short S···S and S···H interstack contacts were observed. Dication–anion interaction is suggested by the short distances between S(7)–H(9), S(10)–H(10), and S(10)–H(12) of 2.78, 2.86, and 2.77 Å, respectively: these are shorter than the sum of the van der Waals radii of 3.00 Å (Figure 7). Considering only the anion arrangement, it is best described as fishbone pattern of dithiolene metalate columns, as also observed for other [Ni(dmit)$_2$]$^-$ complexes. Multiple interstack interactions are indicated by short S···S distances of 3.61 Å (thiolate–thioketone), 3.65 Å (thioketone–thioketone), and of 3.65–3.55 Å (thiolate–thiolate).

0947-6539/01/0703-0742 $ 17.50+.50/0 *Chem. Eur. J.* **2001**, *7*, No. 3

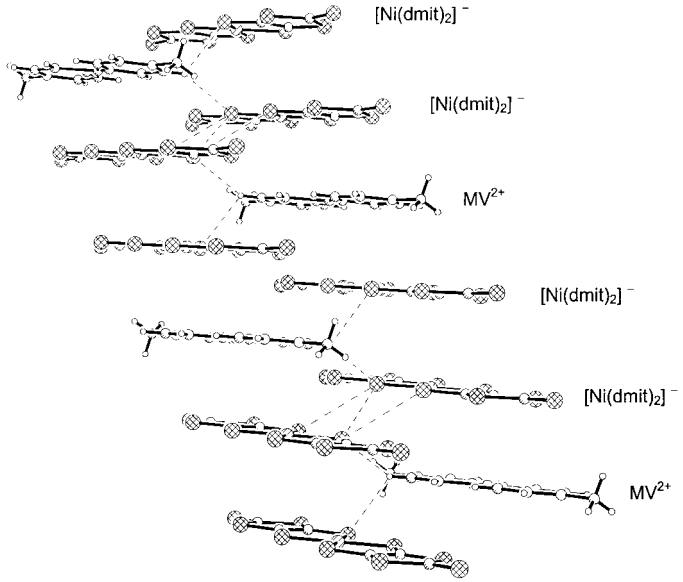

Figure 6. Ion stacking in $MV[Ni(dmit)_2]_2$.

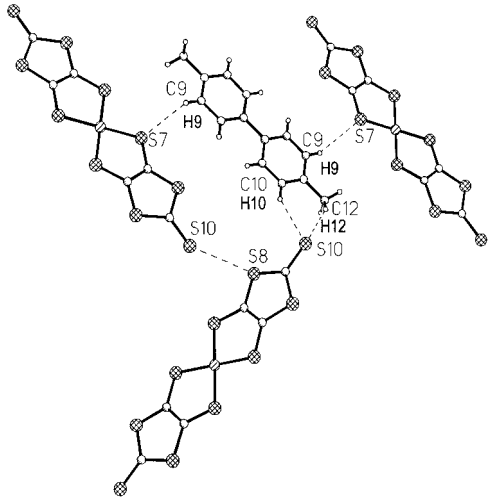

Figure 7. Short interstack distances in $MV[Ni(dmit)_2]_2$.

Electrical conductivity: The specific electrical conductivity of the pressed powder pellets depends on the nature of cation and dithiolene ligands. The dominating influence of the ligand in the absence of any counterion is nicely reflected by the different conductivities of the neutral complexes $[NiL_2]$, which in general are better conductors than the corresponding anionic compounds. In contrast to $dmit^{2-}$ ($3.5 \times 10^{-3}\ \Omega^{-1}\,cm^{-1}$)[35] and $mtdt^{2-}$ (= 1,2-bis(methylthio)-1,2-dithiolate) ($1 \times 10^{-7}\ \Omega^{-1}\,cm^{-1}$),[25] the sterically demanding $diotte^{2-}$ ligand induces a significantly lower value of $3.6 \times 10^{-8}\ \Omega^{-1}\,cm^{-1}$ as measured for $[Ni(diotte)_2]$. Accordingly, the conductivity increased to $2.3 \times 10^{-6}\ \Omega^{-1}\,cm^{-1}$ when one $diotte^{2-}$ ligand was replaced by $dmit^{2-}$ affording the heteroleptic [Ni(diotte)(dmit)].

The conductivity of the diotte/ion-pair complexes $A[Ni(diotte)_2]_2$ increases from $3.2 \times 10^{-10}\ \Omega^{-1}\,cm^{-1}$ for $A^{2+} = MV^{2+}$ to 3.0×10^{-7} and $3.2 \times 10^{-7}\ \Omega^{-1}\,cm^{-1}$ for $A^{2+} = OV^{2+}$ and StV^{2+}, respectively, (Table 3; OV = octyl viologen, StV = stearyl viologen). However, upon the same variation of A^{2+} the conductivity of $A[Ni(dmit)_2]_2$ decreases from $3.9 \times 10^{-6}\ \Omega^{-1}\,cm^{-1}$ to 3.5×10^{-7} and $1.8 \times 10^{-7}\ \Omega^{-1}\,cm^{-1}$.[30] This difference in the steric effect of A^{2+} suggests that the solid-state structure is different for dmit and diotte complexes.

In the range of 293–393 K the temperature dependence of σ follows an Arrhenius behavior, which is diagnostic for an electronic semiconductor. Activation energies (E_a) are in the range of 0.14–0.93 eV. For structurally related ion pairs $\log\sigma$ increases linearly with decreasing E_a as shown in Figure 8 (Table 3). From this relation one can conclude that changes in conductivity reflect changes of E_a and not of the preexponential factor,[36, 37] as also recently observed for the IPCT complexes of the type $A^{2+}[M(dmit)_2]^{2-}$.[2] In contrast to the latter, which all contain a dianionic metal dithiolene, no simple relation between $\log\sigma$ and the driving force of electron transfer from the anion to the cation (ΔG_{12}) is apparent. For instance, although the methyl and octyl viologen salts of $[Ni(diotte)_2]^-$ have almost the same ΔG_{12} values of +0.85 and +0.84 eV (Table 3), the corresponding conductivities are 3.2×10^{-10} and $3.0 \times 10^{-7}\ \Omega^{-1}\,cm^{-1}$, respectively. This suggests that charge generation does not occur by electron transfer, but rather through disproportionation of the monoanions as also proposed for related $[Ni(mnt)_2]^-$ complexes with non-redox-active counter ions.[38] In fact, in the series HiBV[Ni(diotte)L]$_2$ the decrease of disproportionation energy, $\Delta G_{disp} = -nF\{(E_{1/2}(D^{-/2-}) - E_{1/2}(D^{0/-})\}$, from 0.98 eV to 0.94

Table 3. Reduction potentials of ion–pair components, driving force of electron transfer (ΔG_{12}), disproportionation free enthalpies(ΔG_{disp}) electrical parameters ($\log\sigma$, E_a), and onset of the lowest energy band of the solid ion pair (E_{on}).

	E ($D^{0/-}$) [V][a]	E ($D^{-/2-}$) [V][a]	E ($A^{2+/+}$) [V][a]	ΔG_{12} [eV]	$\log\sigma$[b]	E_a [eV]	ΔG_{disp} [eV]	E_{on} [eV]
$MV[Ni(diotte)_2]_2$	+0.42	−0.56	−0.43	+0.85	−9.49	0.41	0.98	0.93
$OV[Ni(diotte)_2]_2$	+0.42	−0.56	−0.42	+0.84	−6.52	0.26	0.98	0.89
$StV[Ni(diotte)_2]_2$	+0.42	−0.56	−0.46	+0.88	−6.49	0.26	0.98	0.87
$HiBV[Ni(diotte)_2]_2$	+0.42	−0.56	−0.41	+0.83	−9.72	0.47	0.98	0.89
$DQ[Ni(diotte)_2]_2$	+0.42	−0.56	−0.36	+0.78	−9.49	0.43	0.98	0.89
$DP[Ni(diotte)_2]_2$	+0.42	−0.56	−0.32	+0.74	−8.41	0.37	0.98	0.93
$HiBV[Ni(diotte)(dmit)]_2$	+0.34	−0.34	−0.41	+0.75	−7.68	0.37	0.68	0.86
$HiBV[Ni(diotte)(mnt)]_2$	+0.74	−0.20	−0.41	+1.15	−9.50	0.43	0.94	0.86
$[(S,S)\text{-HiBV}][Ni\{(R,R)\text{-diotte}\}_2]_2$	+0.42	−0.56	−0.41	+0.83	−10.96	0.67	0.98	0.88
$[(R,R)\text{-HiBV}][Ni\{(R,R)\text{-diotte}\}_2]_2$	+0.42	−0.56	−0.41	+0.83	−12.21	0.93	0.98	0.91
$[(S,S)\text{-HiBV}][Ni\{(S,S)\text{-diotte}\}_2]_2$	+0.42	−0.56	+0.41	+0.83	−11.89	0.89	0.98	0.89
$[(R,R)\text{-HiBV}][Ni\{(S,S)\text{-diotte}\}_2]_2$	+0.42	−0.56	+0.41	+0.83	−10.80	0.63	0.98	0.87
$[Ni(diotte)_2]$	+0.42	–	–	–	−7.44	0.32	–	1.10
[Ni(diotte)(dmit)]	+0.34	–	–	–	−5.64	0.14	–	0.94

[a] From cyclic voltammetry in CH_3CN vs SCE; [b] σ in $\Omega^{-1}\,cm^{-1}$.

  0947-6539/01/0703-0743 $ 17.50+.50/0

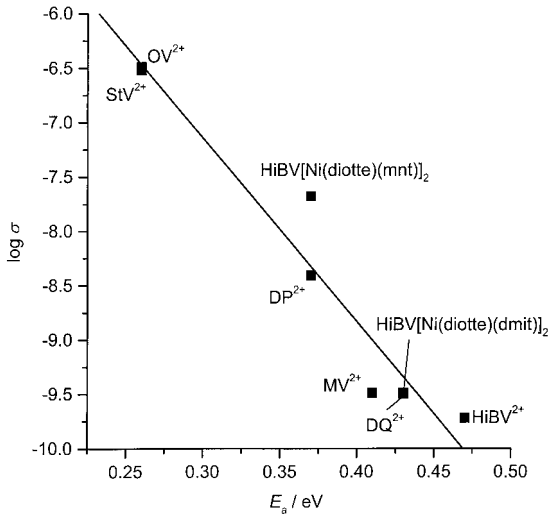

Figure 8. Plot of the logarithm of the specific electrical conductivity as function of the activation energy E_a of A[Ni(diotte)$_2$]$_2$, $A^{2+} = MV^{2+}$, OV^{2+}, StV^{2+}, DP^{2+}, DQ^{2+}, $HiBV^{2+}$, and of HiBV[Ni(diotte)L]$_2$, L = mnt^{2-}, $dmit^{2-}$.

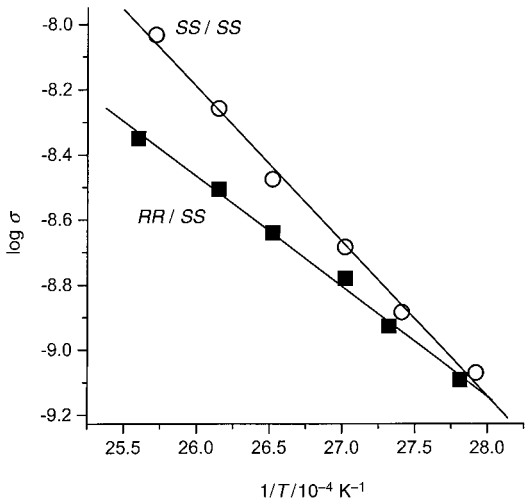

Figure 9. Plot of the logarithm of the specific electrical conductivity as function of $1/T$ for [(*S*,*S*)-HiBV][Ni{(*S*,*S*)-diotte}$_2$]$_2$ and [(*R*,*R*)-HiBV]-[Ni{(*S*,*S*)-diotte}$_2$]$_2$.

to 0.68 eV is accompanied by an increase of conductivity from $1.9 \times 10^{-10}\ \Omega^{-1}\,cm^{-1}$ to 3.2×10^{-10} to $2.0 \times 10^{-8}\ \Omega^{-1}\,cm^{-1}$, respectively. Thus, upon substituting $diotte^{2-}$ by the planar and sterically less demanding mnt^{2-} and $dmit^{2-}$ ligands, electronic rather than steric effects seem to dominate.

When the racemic $diotte^{2-}$ ligand in [Ni(diotte)$_2$] was replaced by the corresponding enantiomers, the conductivities of $1.7 \times 10^{-8}\ \Omega^{-1}\,cm^{-1}$ and $1.6 \times 10^{-8}\ \Omega^{-1}\,cm^{-1}$, as measured for the resulting enantiomeric complexes [Ni{(*R*,*R*)-diotte}$_2$] and [Ni{(*S*,*S*)-diotte}$_2$], respectively, are identical within experimental error. In the case of the complexes with a monoanionic nickel dithiolene, however, the presence of the chiral $HiBV^{2+}$ generates diastereomers that have different conductivities. Whereas again enantiomers like [(*S*,*S*)-HiBV][Ni{(*R*,*R*)-diotte}$_2$]$_2$ and [(*R*,*R*)-HiBV][Ni{(*S*,*S*)-diotte}$_2$]$_2$ exhibit the same conductivities (1.1×10^{-11} and $1.6 \times 10^{-11}\ \Omega^{-1}\,cm^{-1}$, Table 3), their corresponding diastereomers [(*S*,*S*)-HiBV][Ni{(*S*,*S*)-diotte}$_2$]$_2$ and [(*R*,*R*)-HiBV]-[Ni{(*R*,*R*)-diotte}$_2$]$_2$ exhibit values which are smaller by one and two orders of magnitude (1.3×10^{-12} and $6.2 \times 10^{-13}\ \Omega^{-1}\,cm^{-1}$, respectively). This difference is also evident from the activation energies of the two enantiomeric pairs [(*S*,*S*)-HiBV][Ni{(*R*,*R*)-diotte}$_2$]$_2$/[(*R*,*R*)-HiBV][Ni{(*S*,*S*)-diotte}$_2$]$_2$ and [(*R*,*R*)-HiBV][Ni{(*R*,*R*)-diotte}$_2$]$_2$/[(*S*,*S*)-HiBV][Ni{(*S*,*S*)-diotte}$_2$]$_2$ which are 0.67/0.63 and 0.93/0.89 eV, respectively. In Figure 9 the temperature dependence of the conductivity is shown for the two diastereomeric complexes [(*S*,*S*)-HiBV]-[Ni{(*S*,*S*)-diotte}$_2$]$_2$ and [(*R*,*R*)-HiBV][Ni{(*S*,*S*)-diotte}$_2$]$_2$. In summary, the presence of chiral components in these 1:2 ion pairs leads to a decrease of conductivity by one to three orders of magnitude relative to the racemic complex. The conductivity of diastereomers that have components with unlike configurations is one to two orders of magnitude higher than those with like configurations.

Conclusion

Racemic and enantiomerically pure monoanionic dithiolene nickelates and dicationic viologens were combined to 1:2 ion-pair complexes. In contrast to the previously reported 1:1 pairs formed from the corresponding dianions and dications, no evidence for an ion-pair charge-transfer interaction could be found, and the electrical conductivity did not depend on the driving force of anion-to-cation electron transfer, but rather on the disproportion energy of the dithiolene nickelate monanion. The conductivity of diastereomeric complexes differed by one to two orders of magnitude.

Experimental Section

$MVCl_2 \cdot 3H_2O$ (Fluka), $NiCl_2 \cdot 6H_2O$ (Merck), NBu_4Br (Fluka), NH_4PF_6 (Fluka), KOEt (Merck), $P(OEt)_3$ (Fluka), $Hg(OAc)_2$ (Merck), 4,4′-bipyridyl (Fluka), (+)-[(*4R*,*5R*)-4,5-bis(tosyloxymethyl))-2,2-dimethyl-1,3-dioxolane] (Fluka), (−)-[(*4S*,*5S*)-4,5-bis(tosyloxymethyl))-2,2-dimethyl-1,3-dioxolane] (Fluka), and (*R*)-(−)-, (*S*)-(+)-3-bromo-2-methyl-1-propanol (Aldrich) were commercially available and used without further purification. The compounds D,L-4,5-bis(tosyloxymethyl)-2,2-dimethyl-1,3-dioxolane,[11] D,L-,(−)[(*4R*,*5R*)]-, (+)[(*4S*,*5S*)-4,5-bis(bromomethyl)-2,2-dimethyl-1,3-dioxolane],[8] (OV)Br_2,[39] (StV)Br_2,[30] (DQ)Br_2,[40] (DP)Br_2,[41a] MV[Ni(dmit)$_2$]$_2$,[30] NBu_4[Ni(dmit)$_2$],[6] $(NBu_4)_2$[Zn(dmit)$_2$],[6] and $(NBu_4)_2$[Zn(dmid)$_2$],[7] were prepared according to literature methods. Syntheses of the new compounds were performed under aerobic conditions unless otherwise stated. All solvents were dried by standard techniques prior to use.

[(*S*,*S*)-(+)-HiBV]Br_2 and [(*R*,*R*)-(−)-HiBV]Br_2: A solution of 4,4′-bipyridyl (1.80 g, 11.5 mmol) and of (*R*)-(−)-3-bromo-2-methyl-1-propanol (4.36 g, 28.5 mmol) in dry DMF (15 mL) was stirred at 135 °C for 24 h under a nitrogen atmosphere. After cooling to room temperature the yellow precipitate was collected by filtration, washed with dry acetone and dried in high vacuo. Yield 3.44 g (65 %) of **[(*S*,*S*)-(+)-HiBV]Br_2**: Yellow powder; m.p. 248–250 °C (decomp); elemental analysis calcd (%) for $C_{18}H_{26}Br_2N_2O_2$: C 46.77, H 5.67, N 6.06; found: C 46.51, H 5.83, N 5.95; IR (KBr): $\tilde{\nu}$ = 3370 (br m, OH), 1632, 1551, 1502 (s, C=CAr), 826 cm^{-1} (s, γCHAr); UV/Vis (CH_3OH): λ_{max} (ε) = 267 nm (21 000 $M^{-1}\,cm^{-1}$); $[\alpha]_D^{22}$ = +5.4 ± 0.3 (c = 0.9 in CH_3OH); $[\alpha]_{546}^{22}$ = +11.3 ± 0.5 (c = 1.0 in CH_3OH).

[(*R*,*R*)-(−)-HiBV]Br_2: The enantiomer [(*R*,*R*)-(−)-HiBV]Br_2 was obtained as described above in 50 % yield as bright yellow powder; elemental analysis calcd (%) for C 46.49, H 5.82, N 5.95; $[\alpha]_D^{22} = -5.5 \pm 0.4°$ (c = 1.1 in CH_3OH); $[\alpha]_{546}^{22} = -10.9 \pm 0.5°$ (c = 1.0 in CH_3OH); CD spectra of the enantiomers in MeOH ($c = 0.433 \times 10^{-3}$ M) exhibited maxima at 214, 256, and 290 nm.

0947-6539/01/0703-0744 $ 17.50+.50/0 *Chem. Eur. J.* **2001**, *7*, No. 3

[(*S,S*)-(+)-HiBV](PF$_6$)$_2$ and [(*R,R*)-(−)HiBV](PF$_6$)$_2$: NH_4PF_6 (2.1 g, 13 mmol) dissolved in water (5 mL) was added to a solution of (SS(+)-HiBV)Br_2 (3.0 g, 6.5 mmol) in water (20 mL). The flake-like precipitate was collected by filtration after 1 h, washed three times with methanol and dried in high vacuum.

[(*S,S*)-(+)-HiBV](PF$_6$)$_2$: Yield 1.38 g (36 %) of slightly orange colored powder; m.p. 205–207 °C (decomp); elemental analysis calcd (%) for $C_{18}H_{26}F_{12}N_2O_2P_2$: C 36.50, H 4.42, N 4.73, found C 36.54, H 4.48, N 4.61; IR (KBr): $\tilde{\nu}$ = 3617 (m), 3408 (m, OH), 1636 (s), 1558, 1506 (m, C=CAr), 827 (s, γCHAr), 557 cm^{-1} (s, PF); ^{1}H NMR ([D$_6$]acetone): δ = 1.09/1.16 (dd, J = 7.0 Hz, 6H), 2.55/2.85 (m, J = 5.0 Hz, 2H), 4.92 (m, J = 7.0/7.5 Hz, 4H), 8.80 (d, J = 9.0 Hz, 4H; β-ArH), 9.35 (d, J = 9.0 Hz, 4H; α-ArH); ^{13}C NMR ([D$_6$]acetone): δ = 14.1/14.2 (CH_3), 35.8 (CH_2), 38.5 (CH), 64.1 (CH_2OH), 127.8/128.2 (β/β′-Ar), 146.9/147.2 (α′/α-Ar), 150.9/151.4 (γ′/γ-Ar); UV/Vis (CH_3CN): λ_{max} (ε) = 264 nm (25000 M^{-1}cm^{-1}).

(*R,R*(-)HiBV)(PF$_6$)$_2$: Yield 14 %; elemental analysis calcd (%) for C 36.83, H 4.13, N 5.01.

Compound 1: $(NBu_4)_2[Zn(dmit)_2]$ (1.32 g, 1.40 mmol) and D,L-4,5-bis(bromomethyl)-2,2-dimethyl-1,3-dioxolane (1.01 g, 3.51 mmol) were dissolved in dry analytical grade DMF (40 mL) and stirred at 135 °C for 2 h. The solvent was removed completely under reduced pressure, and the viscous residue was purified by flash column chromatography on silica gel (Kieselgel 60, 230–400 mesh) with diethyl ether, followed by recrystallization from ethanol (50 mL). Yield 555 mg (61 %) of a dark orange powder; m.p. 162 °C; elemental analysis calcd (%) for $C_{10}H_{12}O_2S_5$: C 37.02, H 3.73, S 49.40; found C 37.20, H 3.68, S 49.65; IR (KBr): $\tilde{\nu}$ = 2981, 2922 (m), 2880 (w, CH), 1451, 1425, 1404 (m, δasCH), 1379, 1368 (s, δsCH), 1259, 1205, 1168, 1045 (s, C–O), 1065/45 (s, C=S), 962 (w, C-O-C cycl), 878 cm^{-1} (s, C–S); ^{1}H NMR ($CDCl_3$): δ = 1.39 (s, CH_3, 6H), 2.69 (dd, ^{AX}J = 13.9 Hz, ^{AM}J = 10.2 Hz, 2H; H^A), 3.30 (dd, ^{AX}J = 13.9 Hz, ^{MX}J = 3.0 Hz, 2H; H^X), 4.21 (dd, ^{AM}J = 10.2 Hz, ^{MX}J = 3.0 Hz, 2H; H^M); ^{13}C NMR ($CDCl_3$): δ = 26.6 (CH_3), 37.9 (CH_2), 80.3 (CH), 110.4 ($C(CH_3)_2$), 140.8 (C=C), 211.2 (C=S); UV/Vis (CH_2Cl_2): λ_{max} (ε) = 367 (15400), 269 (2500), 224 nm (7800 M^{-1}cm^{-1}).

Compound 2: *Method A*: A solution of $(NBu_4)_2[Zn(dmid)_2]$ (1.25 g, 1.37 mmol) and D,L-4,5-bis(bromomethyl)-2,2-dimethyl-1,3-dioxolane (1.02 g, 3.54 mmol) in dry analytical grade DMF (40 mL) were stirred at 135 °C for 6 h. The crude product was isolated and purified by the same procedure as described above using dichloromethane as eluent. Yield 559 mg (66 %) of orange needles; m.p. 174 °C; elemental analysis calcd (%) for $C_{10}H_{12}O_3S_4$: C 38.94, H 3.92, S 41.58; found C 39.13, H 4.09, S 41.54; IR (KBr): $\tilde{\nu}$ = 2987, 2925 (m), 2889 (w, CH), 1658 (s, C=O), 1453, 1424, 1409 (m, δasCH), 1378, 1369 (s δsCH), 1259, 1211, 1161, 1048 (s, C–O), 962 (w, C-O-C cycl), 881 (s C–S); ^{1}H NMR ($CDCl_3$): δ = 1.40 (s, CH_3, 6H), 2.67 (dd, ^{AX}J = 13.8 Hz, ^{AM}J = 9.7 Hz, 2H; H^A), 3.29 (dd, ^{AX}J = 13.8 Hz, ^{MX}J = 3.2 Hz, 2H; H^X), 4.20 (dd, ^{AM}J = 9.7 Hz, ^{MX}J = 3.2 Hz, 2H; H^M); ^{13}C NMR ($CDCl_3$): δ = 26.8 (CH_3), 37.8 (CH_2), 80.6 (CH), 110.0 ($C(CH_3)_2$), 132.4 (C=C), 188.5 (C=O); UV/Vis (CH_2Cl_2): λ_{max} (ε) = 499 (70), 267 (6000), 222 nm (3800 M^{-1}cm^{-1}).

Method B: A warm solution of $Hg(OAc)_2$ (3.5 g, 11.0 mmol) in glacial acetic acid (100 mL) was added to **1** (3.1 g, 9.55 mmol) dissolved in chloroform (150 mL). The mixture was stirred at 60 °C for 5 h. After cooling to room temperature anhydrous Na_2SO_4 (10 g) was added and the dark precipitate (HgS) was filtered off carefully by suction. Subsequently the residue was extracted three times with hot chloroform, and the combined organic filtrates were neutralized with an aqueous solution of Na_2CO_3 and dried over anhydrous $MgSO_4$. The solvent was removed completely after filtration, and the residue was recrystallized from ethanol (90 mL). Yield 2.28 g (77 %) of an orange powder; elemental analysis calcd (%) for $C_{10}H_{12}O_3S_4$: C 38.94, H 3.92, S 41.58; found C 38.92, H 3.95, S 41.34.

Compound (*4R,5R*)-2: Compound (*4R,5R*)-**2** was prepared by Method A described for **2**, but with the *4R,5R* enantiomer of the dioxolane derivative. Orange needles of (*4R,5R*)-**2**; yield 68 %; elemental analysis calcd (%) for $C_{10}H_{12}O_3S_4$: C 38.94, H 3.92, S 41.58; found C 39.07, H 4.14, S 41.63; $[\alpha]_D^{28}$ = +63 ± 1.5° (c = 1.05 in $CHCl_3$); $[\alpha]_{546}^{22}$ = +72 ± 1.0° (c = 1.0 in $CHCl_3$).

Compound (*4S,5S*)-2: Compound (*4S,5S*)-**2** was prepared analogously to (*4R,5R*)-**2**, but from the *4S,5S* enantiomer of the dioxolane compound. Orange needles, yield 74 %; elemental analysis calcd (%) for for $C_{10}H_{12}O_3S_4$: C 38.94, H 3.92, S 41.58; found C 39.18, H 4.07, S 41.41; $[\alpha]_D^{28}$ = −74.7 ± 0.7° (c = 0.8 in $CHCl_3$); $[\alpha]_{546}^{22}$ = −85.5 ± 0.5° (c = 1.0 in $CHCl_3$).

Compound 3: Compound **2** (300 mg, 0.97 mmol) was added to $P(OEt)_3$ (15 mL) under nitrogen atmosphere, and the mixture was heated up slowly to 110 °C. The resulting orange solution was stirred for 1 h at 110 °C. After cooling to room temperature the mixture was stored at 0 °C for 1 h to complete crystallization. Finally the product was collected by filtration, washed three times with 10 mL of diethyl ether, and dried in high vacuum under exclusion of light. Yield 194 mg (68 %) of an orange powder; m.p. 295–296 °C; elemental analysis calcd (%) for $C_{20}H_{24}O_4S_8$: C 41.07, H 4.14, S 43.85; found C 41.16, H 4.20, S 43.87; IR (KBr): $\tilde{\nu}$ = 2985, 2925 (m), 2890 (w, CH), 1489, 1452 (w), 1411 (m, δasCH), 1379, 1368 (m, δsCH), 1260, 1209, 1161, 1049 (s, C–O), 962 (w, C-O-C), 880 cm^{-1} (s, C–S); ^{1}H NMR ($CDCl_3$): δ = 1.40 (s, CH_3, 6H), 2.63 (dd, ^{AX}J = 12.9 Hz, ^{AM}J = 10.1 Hz, 2H; H^A), 3.25 (dd, ^{AX}J = 12.9 Hz, ^{MX}J = 2.9 Hz, 2H; H^X), 4.21 (dd, ^{AM}J = 10.1 Hz, ^{MX}J = 2.9 Hz, 2H; H^M); ^{13}C NMR ($CDCl_3$): δ = 26.9 (CH_3), 37.3 (CH_2), 80.8 (CH), 108.3 (C=C), 109.9 ($C(CH_3)_2$), 132.5 (C=C); UV/Vis (CH_2Cl_2): λ_{max} (ε) = 428 (1600), 323 (11500), 310 (13200), 226 nm (14800 M^{-1}cm^{-1}); CV (CH_2Cl_2, SCE) : E_1 = +0.60 V, E_2 = +1.01 V.

K$_2$[diotte]: Compound **2** (266 mg, 0.86 mmol) of was added under an inert atmosphere to KOEt (394 mg, 4.68 mmol) suspended in dry THF (10 mL). The slurry was stirred over night, and the brown-yellow precipitate was isolated by filtration after addition of dry *n*-hexane (5 mL). The product was carefully washed with *n*-hexane and dried in high vacuum. Yield 280 mg (91 %) of an extreme air sensitive beige powder. IR (Nujol mull): $\tilde{\nu}$ = 1663 (s, C=C), 1576 (br s), 1295 (m), 1210 (br m), 1049 (s, C–O), 970 (w, C-O-C), 881 cm^{-1} (w, C–S); ^{13}C NMR ([D$_6$]DMSO): 26.5 (CH_3), 36.9 (CH_2), 77.4 (CH), 105.0 (C=C), 107.8/108.2 ($C(CH_3)_2$).

(NBu$_4$)[Ni(diotte)$_2$]: Compound **2** (535 mg, 1.73 mmol) was added to a solution of KOEt (666 mg, 7.91 mmol) in dry methanol (20 mL) under an inert atmosphere. The suspension was stirred for 3 h at room temperature and then filtered through Celite. $NiCl_2 \cdot 6H_2O$ (214 mg, 0.9 mmol) dissolved in methanol (5 mL) was added dropwise to the dark orange filtrate. After 30 minutes the mixture was filtered again, and the filtrate was combined with a solution of NBu_4Br (548 mg, 1.7 mmol) in methanol (5 mL). Immediately a dark brown precipitate was formed, which was cooled to −20 °C to complete crystallization. The crude product was isolated by filtration and purified by soxhlet extraction with isopropanol and subsequent recrystallization from acetone/isopropanol (2:1, v/v). Yield 388 mg (52 %) of bronze microcrystals; m.p. 214 °C (decomp); elemental analysis calcd (%) for $C_{34}H_{60}NO_4S_8Ni$: C 47.37, H 7.02, N 1.62, S 29.75; found C 47.03, H 7.07, N 1.59, S 29.65; IR (KBr): $\tilde{\nu}$ = 1386 (s, C=C), 880 (s, C–S), 568 cm^{-1} (w, Ni–S); UV/Vis (CH_2Cl_2): λ_{max} (ε) = 886 (8800), 397 (12300), 344 (14300), 303 (14500), 248 nm (25100 M^{-1}cm^{-1}).

(NBu$_4$)[Ni{(*R,R*)-diotte}$_2$] and (NBu$_4$)[Ni{(*S,S*)-diotte}$_2$]: These compounds were prepared by the method desribed for $(NBu_4)[Ni(diotte)_2]$, but from (*4R,5R*)-**2** and (*4S,5S*)-**2**, respectively. $(NBu_4)[Ni\{(R,R)\text{-diotte}\}_2]$: yield 45 %; elemental analysis calcd (%) for $C_{34}H_{60}NO_4S_8Ni$: C 47.37, H 7.02, N 1.62, S 29.75; found C 47.31, H 7.23, N 1.63, S 29.50; $(NBu_4)[Ni\{(S,S)\text{-diotte}\}_2]$: yield 32 %; elemental analysis calcd (%) for $C_{34}H_{60}NO_4S_8Ni$: C 47.37, H 7.02, N 1.62, S 29.75; found C 47.16, H 7.11, N 1.66, S 30.05.

[Ni(diotte)$_2$]: A solution of iodine (250 mg, 0.99 mmol) and NaI (350 mg, 2.33 mmol) in acetone (10 mL) was added to $(NBu_4)[Ni(diotte)_2]$ (1.54 g, 1.79 mmol) dissolved in of acetone (100 mL). The mixture was stirred at room temperature for 30 minutes. The volume was reduced to about 50 mL by rotary evaporation, the resulting blue-green precipitate was filtered off and washed with methanol until colorless filtrates were obtained. Finally the product was dried in high vacuum. Yield 923 mg (84 %) of an olive-green powder; m.p. 288 °C (decomp); elemental analysis calcd (%) for $C_{18}H_{24}O_4S_8Ni$: C 34.89, H 3.90, S 41.40; found C 35.16, H 3.94, S 41.43; IR (KBr): $\tilde{\nu}$ = 1270 (s, C=C), 880 (s, C–S), 587 cm^{-1} (w, Ni–S); UV/Vis (CH_2Cl_2): $\tilde{\nu}$ = 823 (18100), 579 (1600), 391 (32000), 285 (33000), 250 nm (29100 M^{-1}cm^{-1}).

[Ni{(*R,R*)-diotte)$_2$] and [Ni{(*S,S*)-diotte}$_2$]: $[Ni\{(R,R)\text{-diotte})_2]$ was prepared as described for $[Ni(diotte)_2]$, but with $(NBu_4)[Ni\{(R,R)\text{-diotte}\}_2]$. Yield 76 %; elemental analysis calcd (%) for $C_{18}H_{24}O_4S_8Ni$: C 34.89, H 3.90, S 41.40; found C 35.23, H 3.87, S 41.61. $[Ni\{(S,S)\text{-diotte}\}_2]$ was obtained analogously, but from $(NBu_4)[Ni\{(S,S)\text{-diotte}\}_2]$. Yield 74 %; elemental analysis found (%) for $C_{18}H_{24}O_4S_8Ni$: C 34.89, H 3.90, S 41.40; found C 35.01, H 3.90, S 41.53.

(NBu$_4$)[Ni(diotte)(dmit)]: $(NBu_4)_2[Ni(dmit)_2]$ (225 mg, 0.24 mmol) and $[Ni(diotte)_2]$ (150 mg, 0.24 mmol) dissolved in acetone (70 mL) were stirred

at 60 °C for 8 h. After removing the solvent in vacuo, the dark residue was treated with methanol (20 mL), collected by filtration, and subsequently dried in high vacuum. Yield 183 mg (49 %); green brown powder, m.p. 134 °C; elemental analysis calcd (%) for $C_{28}H_{48}NO_2S_9Ni$: C 43.23, H 6.22, N 1.80, S 37.09; found C 43.12, H 6.23, N 1.77, S 37.11; IR (KBr): $\tilde{\nu} = 1368$, 1350 (s, C=C), 1060/35 (s, C=S), 881 (m, C–S), 570 cm^{-1} (w, Ni–S); UV/Vis (CH_2Cl_2): λ_{max} (ε) = 1000 (15 600), 625 (3300), 550 (3100), 434 (21 000), 376 (24 200), 303 nm (31 000 $M^{-1}cm^{-1}$).

(NBu_4)[Ni{(*R*,*R*)-diotte}(dmit)]: This compound was prepared by the method used for (NBu_4)[Ni{(*R*,*R*)-diotte}(dmit)], but from [Ni{(*R*,*R*)-diotte}$_2$]. Yield 88 %; elemental analysis calcd (%) for $C_{28}H_{48}NO_2S_9Ni$: C 43.23, H 6.22, N 1.80, S 37.09; found C 43.47, H 6.36, N 1.86, S 36.79.

[Ni(diotte)(dmit)]: The corresponding neutral complex was prepared by the same procedure as described for [Ni(diotte)$_2$]. Yield 77 %, dark olive-green solid; m.p. > 360 °C; elemental analysis calcd (%) for $C_{12}H_{12}O_2S_9Ni$: C 26.92, H 2.26, S 53.88; found C 27.13, H 2.24, S 53.19; IR (KBr): $\tilde{\nu} = 1270$ (s, C=C), 1066/49 (s, C=S), 898, 878 (m, C–S), 502 cm^{-1} (m, Ni–S); UV/Vis (CH_2Cl_2): $\lambda_{max} = 906$, 629, 404, 293, 247 nm.

(NBu_4)[Ni(diotte)(mnt)]: A solution of $(NBu_4)_2$[Ni(mnt)$_2$] (935 mg, 1.14 mmol) and [Ni(diotte)$_2$] (708 mg, 1.14 mmol) in acetone was stirred at 60 °C for 7 h. The solvent was removed completely, and the dark viscous residue was treated with methanol (60 mL). Subsequently the mixture was filtered, and the dark green filtrate stored at 0 °C over night. A green yellow precipitate formed which was filtered off and dried in high vacuum. Yield 1.14 g (69 %); yellow green powder, m.p. 104 – 106 °C; elemental analysis calcd (%) for $C_{29}H_{48}N_3O_2S_6Ni$: C 48.26, H 6.70, N 5.82, S 26.65; found C 48.14, H 6.74, N 5.89, S 26.43; IR (KBr): $\tilde{\nu} = 2205$ (m, CN), 1379 (s, C=C), 879 (s, C–S), 570 cm^{-1} (w, Ni–S); UV/Vis (CH_2Cl_2): λ_{max} (ε) = 880 (9800), 656 (1200), 520 (1500), 395 (12 400), 310 (23 000), 266 nm (29 300 $M^{-1}cm^{-1}$).

(NBu_4)[Ni{(*R*,*R*)-diotte}(mnt)] and (NBu_4)[Ni{(*S*,*S*)-diotte}(mnt)]: (NBu_4)[Ni{(*R*,*R*)-diotte}(mnt)] was prepared by the procedure derscribed for (NBu_4)[Ni(diotte)(mnt)], but from Ni(*R*,*R*-diotte)$_2$; yield 47 %, dark green needles; elemental analysis calcd (%) for $C_{29}H_{48}N_3O_2S_6Ni$: C 48.26, H 6.70, N 5.82, S 26.65; found C 48.46, H 6.90, N 5.85, S 26.25. (NBu_4)[Ni{(*S*,*S*)-diotte}(mnt)] was prepared analogously but from Ni(*S*,*S*-diotte)$_2$; yield 34 %, dark green needles; elemental analysis calcd (%) for $C_{29}H_{48}N_3O_2S_6Ni$: C 48.26, H 6.70, N 5.82, S 26.65; found: C 48.61, H 6.77, N 5.86, S 26.86.

MV[Ni(diotte)$_2$]$_2$: $(MV)Cl_2 \cdot 3H_2O$ (162 mg, 0.52 mmol) dissolved in methanol (10 mL) was added dropwise to a filtered solution of (NBu_4)[Ni(diotte)$_2$] (900 mg, 1.04 mmol) in acetone/methanol (2:1, v/v, 75 mL) at 40 °C without stirring. Rapidly a dark blue precipitate was formed, which was collected by filtration after 24 h. The microcrystalline solid was carefully washed with methanol and dried in high vacuum. Yield 495 mg (67 %), dark blue crystals, m.p. > 320 °C; elemental analysis calcd (%) for $C_{48}H_{62}N_2O_8S_{16}Ni_2$: C 40.45, H 4.38, N 1.97, S 35.99; found C 40.38, H 4.21, N 1.67, S 36.12

OV[Ni(diotte)$_2$]$_2$, StV[Ni(diotte)$_2$]$_2$, HiBV[Ni(diotte)$_2$]$_2$, DQ[Ni-(diotte)$_2$]$_2$, DP[Ni(diotte)$_2$]$_2$, HiBV[Ni(diotte)(dmit)], HiBV[Ni(diotte)-(mnt)], [(*R*,*R*)-HiBV][Ni{(*R*,*R*)-diotte}$_2$]$_2$, [(*S*,*S*)-HiBV][Ni{(*R*,*R*)-diotte}$_2$]$_2$, [(*R*,*R*)-HiBV][Ni{(*S*,*S*)-diotte}$_2$]$_2$, and [(*S*,*S*)-HiBV][Ni{(*S*,*S*)-diotte}$_2$]$_2$: These compounds were synthesized analogously by metathesis reaction with the corresponding viologen dibromides.

X-ray crystal structure determinations: Orange, single-crystal platelets of (*R*,*R*)-**2** were obtained by dissolving the powder in ethanol at 60 °C and cooling to 0 °C. Data were collected by the ω-scan technique in the range $3 \le 2\theta \le 54°$ on a Siemens R3m/V four-circle diffractometer at 293 K. Unit cell parameters were determined by least-square fits of 18 reflections. The structure was solved by direct methods. All non-hydrogen atoms were refined anisotropically, and the hydrogen atoms of the methyl and methylene groups were included in idealized calculated positions. All calculations were performed by using the SHELXTL-Plus program package.[41c] Significant crystallographic data are summarized in Table 4. Final atomic coordinates with their estimated standard deviations and selected bond lengths and bond angles are available from the Cambridge Crystallogrphic Database (see below).

For the high resolution X-ray powder diffraction experiments, the sample was sealed in a glass capillary of 0.5 mm diameter (Hilgenberg glass No. 50). Powder diffraction data were collected at room temperature at beamline X3B1 at the National Synchrotron Light Source, Brookhaven National Laboratory as reported recently.[1] In the parallel beam geometry employed, the resolution is determined by the analyzer crystal instead of by slits.[42] X-ray scattering intensities were recorded at wavelength 1.15030(2) Å in steps of 0.01° 2θ for 5.1 seconds at each step from 4.0° to 33.99° 2θ and for 10.1 seconds at each step from 34.0° to 59.13° 2θ (Figure 10). The sample was spun around θ during measurement to reduce crystallite-size effects. Lowest angle diffraction peaks had a full width at half maximum (FWHM) of 0.040° 2θ, much broader than the resolution of

Table 4. Crystallographic data for **2** and MV[Ni(dmit)$_2$]$_2$.

Compound	**2**	MV[Ni(dmit)$_2$]$_2$
formula	$C_{10}H_{12}O_3S_4$	$Ni_2S_{20}N_2C_{25}H_8$
M_r [g mol^{-1}]	308.40	2190.10
crystal size [mm]	0.4 × 0.4 × 0.3	powder
F(000)	640	1096
space group	$P2_12_12_1$	$P2_1/a$
crystal system	orthorhombic	monoclinic
a [Å]	10.287(5)	22.338(6)
b [Å]	10.99.9(4)	11.382(3)
c [Å]	11.780(5)	7.537(2)
α [°]	90	90
β [°]	90	98.185(1)
γ [°]	90	90
V [nm^3]	1.333(1)	1.8968(9)
Z	4	2
ρ_{calcd} [g cm^{-3}]	1.537	1.917
μ [mm^{-1}]	0.705	–
diffractometer	Siemens R3m/V	Huber 2-circle
radiation [pm]	$Mo_{K\alpha}$(λ = 71.073)	0.115030(2)
T [K]	293	295
scan technique	σ scan	$\theta/2\theta$
2θ range [°]	3.0 – 54.0	4.0 – 59.13
step width [° 2θ]		0.01
scan speed [sec step^{-1}]	3.00 – 29.30	4.0 – 33.99° 2Θ: 5.1 34.0 – 59.13° 2Θ: 10.1
measured reflections	3251	1262
independent reflections	2940	–
R_{int} [%]	3.35	11.92
observed reflections	1593	–
σ criterion	$F > 4.0\sigma(F)$	–
R_1/wR_2 [%]	0.0625/0.1023	5.40/7.50
refined parameters	155	21

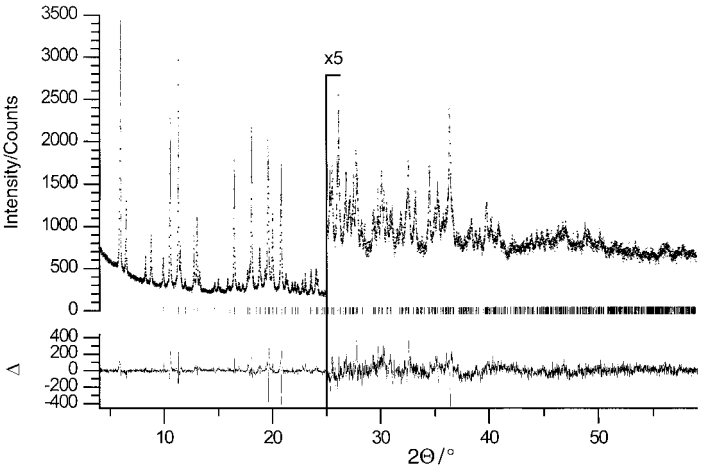

Figure 10. Scattered X-ray intensity for MV[Ni(dmit)$_2$]$_2$ at ambient conditions as a function of diffraction angle 2θ; Top: observed pattern (■) and best Rietveld fit profile (——). The trace at the bottom corresponds to reflection positions and difference curve between observed and calculated profiles. The high angle part is enlarged by a factor of 5 starting at 25° 2θ.

0947-6539/01/0703-0746 $ 17.50+.50/0 *Chem. Eur. J.* **2001**, *7*, No. 3

the diffractometer. Data reduction was performed using the program GUFI 5.0.[43] Indexing of the powder pattern of $MV[Ni(dmit)_2]_2$ with the program ITO[44] led to a primitive monoclinic unit cell with lattice parameters given in Table 4. The number of formula units per unit cell could be determined to $Z=2$ from packing considerations. The space group $P2_1/a$ could be unambiguously determined by applying the extinction rules.

The peak profiles and precise lattice parameters were determined by LeBail-type fits using the program Fullprof.[45] The background was modeled manually using GUFI. The peak-profile was described by a pseudo-Voigt in combination with a special function that accounts for the asymmetry due to axial divergence.[46]

Since the connectivity of the atoms was known from single crystal studies of the two components[31, 47], structure determination for $MV[Ni(dmit)_2]_2$ was carried out by means of the simulated annealing technique.[48–52] For the simulated annealing runs, the program DASH[53] was used. Three input files were needed: a description of the connectivity of the two molecules including possible torsion angles, a list of diffraction peak intensities, and a list of parameters to be varied and their ranges for the simulated annealing runs.

For the definition of the connectivity between the atoms within the $[Ni(dmit)_2]$ and the MV molecules, we used the Z-matrix notation[54a], which allows for the description of the entire molecule and its intramolecular degrees of freedom by using interatomic distances, angles, and dihedral angles. A flag after each parameter determined whether this parameter was included in the simulated annealing process or not. All intramolecular angles and distances were kept fixed at standard values, allowing only the position and orientation of the two molecules to vary.

The diffraction intensities were extracted from a Pawley-type refinement with the program DASH.[53, 55] The peak profile was modeled by the Voigt-function, to which a correction for the asymmetry due to axial divergence was applied. The background was included in the refinement process using high order Chebyshev polynoms. The covariance matrix of the Pawley fit, which describes the degree of correlation between the individual intensities of neighboring reflections, was actively used in the calculation of the level of agreement between the measured intensities and those of the trial structures after each simulated annealing. It was therefore not necessary to include the entire powder pattern in the simulated annealing procedure; this considerably decreased the computing time needed for each cycle.

Since the position of the MV^{2+} molecule could be fixed at the center of symmetry, a total of 11 parameters were varied during the simulated annealing runs (three fractional parameters for the positions of the $[Ni(dmit)_2]$ molecule, and 2×4 quaternians[54b] describing the orientations of the $[Ni(dmit)_2]$ and the MV molecules within the unit cell). The trial structures were generated using a set of numbers chosen randomly in a Monte Carlo fashion within the given range for the 11 parameters.[56] The starting temperature[57] for the simulated annealing run was set to 100 K, and decreased slowly, allowing several thousand moves per temperature. Several million trial structures were generated before this minimum was reached, the process taking a few hours to run on a Digital Personal Workstation 433au. A simplex search at the end of the simulated annealing run confirmed that a deep minimum, corresponding to an approximately correct crystal structure, had been obtained. Note that no special algorithms were employed to prevent close contact of molecules during the global optimization procedure. In general, these have not been found to be necessary as the fit to the structure factors alone quickly moves the molecules to regions of the unit cell where they do not grossly overlap with neighboring molecules.

Preliminary Rietveld[58] refinements were carried out, in which only the scale and overall temperature factors were refined. The agreement between the measured and the calculated profile was already quite satisfactory, indicated that further refinement of bond lengths and bond angles might not reveal more structural details. The coordinates obtained by the simulated annealing techniques were used as starting parameters for Rietveld refinements with the GSAS program system .[59] Since unconstrained refinement resulted in meaningless distortions from the ideal molecular symmetry, two rigid bodies representing the two independent molecules were used. This step reduced the number of refinable parameters for the two molecules to 11 (three translations, 2×3 rotations and 2×1 overall temperature factors). Since the rigid bodies definition in GSAS allows the refinement of selected internal bond lengths, the average Ni–S, S–C, C–C/N bond lengths were refined, while keeping the C–H and the central C–C bond lengths of the MV molecule fixed.

The Rietveld refinement converged quickly to the R values given in the caption of Figure 10. The positions of all non-hydrogen atoms were fully released at the final stage of the refinement process, but did not change significantly, proving that both molecules are flat within the standard deviations. The positional parameters of the final Rietveld refinement (using rigid bodies), the overall temperature factors are available from the Cambridge Crystallographic Database (see below). A selection of bond lengths and angles are presented in Table 1.

Crystallographic data (excluding structure factors) for the structure reported in this paper have been deposited with the Cambridge Crystallographic Data Centre as supplementary publication no. CCDC-140147. Copies of the data can be obtained free of charge on application to CCDC, 12 Union Road, Cambridge CB21EZ, UK (fax: (+44) 1223-336-033; e-mail: deposit@ccdc.cam.ac.uk).

Physical measurements: Melting points are uncorrected and were obtained with an Electrothermal apparatus. Microanalyses were determined with a Carlo Erba Model 1106 elemental analyzer. IR spectra (KBr pellet or Nujol mull) were measured with a Perkin–Elmer Model 983 instrument. ^1H, ^{13}C NMR, and ESR spectra were recorded with Jeol-PMX 60, Jeol FT-JNM-GX-270-NMR, and Bruker ESP 300E (employing 1,1-diphenyl-2-picrylhydrazyl as internal standard, $g=2.0036$) spectrometers, respectively. Optical rotations were recorded with a Schmidt & Haensch Polartronic E Eloptron polarimeter and circular dichroism (CD) spectra with a Jasco spectropolarimeter J600. Diffuse reflectance spectra were measured relative to corundum (Hoechst Ceram Tec) with a Shimadzu Model 3101 spectrophotometer equipped with an integrating sphere unit. The onset of the lowest energy transition E_{on} was determined according to the method by Karvaly and Hevesi[60] as described previously.[2a] Cyclic voltammetry was performed with an EG&G Princeton Applied Research Model 264A potentiostat by using a conventional three-electrode assembly consisting of a glassy-carbon working electrode, a platinum wire as counter electrode, and an Ag/AgCl reference electrode in saturated KCl solution. All measurements were conducted in dry and nitrogen-degassed acetonitrile and dichloromethane solutions (10^{-3} M) containing 0.1M NBu_4PF_6 as supporting electrolyte and ferrocene as internal reference. Potentials were calibrated relative to the ferrocene/ferrocenium redox couple and referenced versus SCE by $E_{1/2}(Fc^{+/0})=0.39$ V.[61] Specific conductivities were obtained by the two-probe method as described previously;[2a, 30] control measurements by the four-probe method afforded values identical within $\pm10\%$;[30] pellets of 0.15–0.85 mm thickness were obtained upon applying a pressure of $9.8\times10\,Nm^{-2}$ for 10 min to the sample, which was dried before in high vacuum for 48 h and ground in an agate mortar; reproducibility of the data was within $\pm$ 15%. Activation energies E_a were determined by transferring the pellet into a Teflon cell containing brass contacts and a Ni/Cr-Ni thermoelement. The cell was immersed into an oil bath and resistivity was measured in the range of 293–393 K; $\log\sigma$ versus $1/T$ plots were linear in all cases.

Acknowledgement

This work was supported by Volkswagen-Stiftung and Fonds der Chemischen Industrie. We are grateful to U. Wagner, University of Dortmund, and Dr. Utz, University of Erlangen-Nürnberg for measuring CD spectra. X-ray powder diffraction measurements were carried out in part at the National Synchrotron Light Source at Brookhaven National Laboratory, which is supported by the US Department of Energy, Division of Materials Sciences, and Division of Chemical Sciences. The SUNY X3 beamline at NSLS is supported by the Division of Basic Energy Sciences of the US Department of Energy under Grant No. DE-FG02–86ER45231. Financial support by the Deutsche Forschungsgemeinschaft (DFG) is gratefully acknowledged.

[1] C. Handrosch, R. Dinnebier, G. Bondarenko, E. Bothe, F. Heinemann, H. Kisch, *Eur. J. Inorg. Chem.* **1999**, 1259.

[2] a) I. Nunn, B.Eisen, R. Benedix, H. Kisch, *Inorg. Chem.* **1994**, *33*, 5079; b) H. Kisch, *Comments Inorg. Chem.* **1994**, *16*, 113.

[3] a) H. Rau, R. Ratz, *Angew. Chem.* **1983**, *95*, 552; *Angew. Chem. Int. Ed. Engl.* **1983**, *22*, 550; b) H. Rau, *Chem. Rev.* **1983**, *83*, 535; c) K. Tsukahara, Ch. Kimura, J. Kaneko, K. Abe, M. Matsui, T. Hara, *Inorg. Chem.* **1997**, *36*, 3520.
[4] J. D. Wallis, A. Karrer, J. D. Dunitz, *Helv. Chim. Acta* **1986**, *69*, 69.
[5] J. S. Zambounis, C. W. Mayer, K. Hauenstein, B. Hilti, W. Hofherr, J. Pfeiffer, M.Bürkle, G. Rihs, *Adv. Mater.* **1992**, *4*, 33.
[6] a) G. Steimecke, R. Kirmse, E.Hoyer, *Z. Chem.* **1975**, *15*, 28; b) G. Steimecke, H. J. Sieler, R. Kirmse, E. Hoyer, *Phosphorus Sulfur Relat. Elem.* **1979**, *7*, 49.
[7] J. Köster, Ph.D. Thesis, Philipps-Universität, Marburg **1983**.
[8] J. M. Townsend, J. F. Blount, R. C. Sun, S. Zawoiski, Jr., D. Valentine, *J. Org. Chem.* **1980**, *45*, 2995.
[9] K. Hartke, T. Kissel, J. Quante, R. Matusch, *Chem. Ber.* **1980**, *113*, 1898.
[10] B. Eisen, H. Kisch, unpublished results.
[11] B. A. Murrer, J. M. Brown, P. A. Chaloner, P. N. Nicholson, D. Parker, *Synthesis* **1979**, 350.
[12] F. Grasser, Ph.D. Thesis, University of Erlangen-Nürnberg, **1991**.
[13] H. Poleschner, W. John, F. Hoppe, E. Fanghänel, *J. Prakt. Chem.* **1983**, *325*, 957.
[14] a) H. D. Hartzler, *J. Am. Chem. Soc.* **1973**, *95*, 4379; b) M. G. Miles, J. D. Wilson, D. J. Dahn, J. H. Wagenknecht, *J. Chem. Soc. Chem. Commun.* **1974**, 751; c) S. Yoneda, T. Kawase, M. Inaba, Z. Yoshida, *J. Org. Chem.* **1978**, *43*, 595; d) M. R. Bryce, *Aldrichimica Acta* **1985**, *18*, 73.
[15] E. M. Engler, V. Y. Lee, R. R. Schumaker, S. S. P. Parkin, R. L. Greene, J. C. Scott, *Mol. Cryst. Liq. Cryst.* **1984**, *107*, 19.
[16] J. Röhrich, P. Wolf, V. Enkelmann, K. Müllen, *Angew. Chem.* **1988**, *100*, 1429; *Angew. Chem. Int. Ed. Engl.* **1988**, *27*, 1377.
[17] J. Fabian, E. Fanghänel, *J. Prakt. Chem.* **1967**, *36*, 287.
[18] R. Mayer, P. Gebhardt, *Chem. Ber.* **1964**, *97*, 1298.
[19] a) C. T. Vance, R. D. Bereman, J. Bordner, W. E. Hatfield, J. H. Helms, *Inorg. Chem.* **1985**, *24*, 2905; b) J. H. Welch, R. D. Bereman, P. Singh, *Inorg. Chem.* **1988**, *27*, 3680; c) J. H. Welch, R. D. Bereman, P. Singh, D. Haase, W. E. Hatfield, M. L. Kirk, *Inorg. Chim. Acta* **1989**, *162*, 89; d) C. T. Vance, R. D. Bereman, *Inorg. Chim. Acta* **1988**, *149*, 229.
[20] a) R. Kato, H. Kobayashi, A. Kobayashi, Y. Sasaki, *Bull. Chem. Soc. Jpn.* **1986**, *59*, 627; b) T. Nakamura, T. Nogami, Y. Shirota, *Bull. Chem. Soc. Jpn.* **1987**, *60*, 3447.
[21] R.-M. Olk, W. Dietzsch, K. Köhler, R. Kirmse, J. Reinhold, E. Hoyer, L. Golic, B. Olk, *Z. Anorg. Allg. Chem.* **1988**, *567*, 131.
[22] A. Fernandez, Ph.D. Thesis, University of Dortmund, **1984**.
[23] J. Spanget-Larsen, R. Gleiter, M. Kobayashi, E. M. Engler, P. Shu, D. O. Cowan, *J. Am. Chem. Soc.* **1977**, *99*, 2855.
[24] McCleverty, *Prog. Inorg. Chem.* **1968**, *10*, 49.
[25] C. Kraffert, D. Walther, K. Peters, O. Lindquist, V. Langer, J. Sieler, J. Reinhold, E. Hoyer, *Z. Anorg. Allg. Chem.* **1990**, *588*, 167.
[26] U. T. Mueller-Westerhoff, B. Vance, *Comprehensive Coordination Chemistry*, Oxford, **1987**, p. 595.
[27] A. Vogler, H. Kunkely, J. Hlavatsch, A. Merz, *Inorg. Chem.* **1984**, *23*, 506.
[28] A. H. Maki, N. Edelstein, A. Davison, R. H. Holm, *J. Am. Chem. Soc.* **1964**, *86*, 4580.
[29] E. Hoyer, W. Dietzsch, W. Schroth, *Z. Chem.* **1971**, *11*, 41.
[30] F. Nüßlein, R. Peter, H. Kisch, *Chem. Ber.* **1989**, *122*, 1023.
[31] O. Lindquist, L. Andersen, J. Sieler, G. Steimecke, E. Hoyer, *Acta Chem. Scand.* **1982**, *36*, 855.
[32] I. Malfant, R. Andreu, P. G. Lacroix, C. Faulmann, P. Cassoux, *Inorg. Chem.* **1998**, *37*, 3361.
[33] L. Valade, J.-P. Legros, M. Bousseau, P. Cassoux, *J. Chem. Soc. Dalton Trans.* **1985**, 783.
[34] Sh. Sun, P. Wu, D. Zhu, *Synth. Met.* **1997**, *88*, 243.
[35] a) L. Valade, M. Bousseau, A. Gleizes, P. Cassoux, *J. Chem. Soc. Chem. Commun.* **1983**, 110; b) L. Valade, J. P. Legros, M. Bousseau, P. Cassoux, M. Garbauskas, L. V. Interrante, *J. Chem. Soc. Dalton Trans.* **1985**, 783.
[36] K. Ulbert, *J. Polymer. Sci. C* **1969**, *27*, 881.
[37] H. Meier, *Organic Semiconductors: Dark- and Photoconductivity of Organic Solids*, VCH, Weinheim, **1974**.
[38] D. R. Rosseinsky, R. E. Malpas, *J. Chem. Soc. Dalton Trans.* **1979**, 749.
[39] R. Maidan, Z. Goren, J. Y. Becker, I. Willner, *J. Am. Chem. Soc.* **1984**, *106*, 6217.
[40] R. F. Homer, T. E. Tomlinson, *J. Chem. Soc.* **1960**, 2498.
[41] a) S. Hünig, J. Gross, E. F. Lier, H. Quast, *Liebigs Ann. Chem.* **1973**, 339; b) L. A. Summers, V. A. Pickles, *Chem. Ind.* **1967**, 619; c) G. M. Sheldrick, *SHELXTL Plus, Structure Determination Software Programs*, Siemens Analytical X-ray Instruments, Madison, WI, **1990**.
[42] a) D. E. Cox, *Handbook on Synchrotron Radiation*, *Vol. 3* (Eds.: G. Brown, D. E. Moncton), Elsevier Science, **1991**, Chapter 5; b) I. Langford, D. Louër, *Rep. Prog. Phys.* **1996**, *59*, 131.
[43] R. E. Dinnebier, L. W. Finger, *Z. Kristallogr. Suppl.* **1998**, *15*, 148.
[44] J. W. Visser, *J. Appl. Cryst.* **1969**, *2*, 89.
[45] J. Rodriguez-Carvajal, *Abstracts of Papers*, Satellite Meeting on Powder Diffraction of the *XV Congress of the IUCR*, Toulouse, France, **1990**, Abstract 127.
[46] L. W. Finger, D. E. Cox, A. P. Jephcoat, *J. Appl. Cryst.* **1994**, *27*, 892.
[47] J. Russel, S. C. Wallwork, *Acta Crystallogr. Sect. B* **1972**, *28*, 1527; see also ref. [2b].
[48] P. J. M. van Laarhoven, E. H. L. Aarts, *Simulated Annealing: Theory and Applications*, D. Reidel Publishing Company, Dordrecht, **1987**.
[49] J. M. Newsam, M. W. Deem, C. M. Freeman, *Accuracy in Powder Diffraction II*, *NIST Spec. Publ. No. 846* **1992**, 80.
[50] Y. G. Andreev, G. S. MacGlashan, P. G. Bruce, *Phys. Rev. B* **1997**, *55*, 12011.
[51] W. I. F. David, K. Shankland, N. Shankland, *Chem. Commun.* **1998**, 931.
[52] G. S. Macglashan, Y. G. Andreev, P. G. Bruce, *Nature* **1999**, *398*, 792.
[53] W. I. F. David, simulated annealing program DASH **1999**, personal communication.
[54] a) A. R. Leach, *Molecular Modelling Principles and Applications*, Longman, **1996**, p. 2. b) The four quaternians allow a uniform sampling over the surface of a sphere in contrast to the three Euler angles.
[55] G. S. Pawley, *J. Appl. Crystallogr.* **1981**, *14*, 357.
[56] W. H. Press, S. A. Teukolsky, W. T. Vetterling, B. P. Flannery, *Numerical Recipes in Fortran 77*, 2nd ed., Cambridge University Press, **1992**.
[57] This is not a temperature in thermodynamical sense, but refers to the term T in the expression $\exp(E/KT)$ which is generally known Boltzmann factor with the Boltzmann constant K and the state of energy E. The analogous experession with $E=\chi^2_{\mathrm{new}}-\chi^2_{\mathrm{new}}$ (difference in χ^2 of consecutive cycles) is used as an acceptance criterion in the simulated annealing process.
[58] H. M. Rietveld, *J. Appl. Crystallogr.* **1969**, *2*, 65.
[59] A. C. Larson, R. B. Von Dreele, "*GSAS—General Structure Analysis System*", Los Alamos National Laboratory Report LAUR 86–748 **1994**, available by anonymous FTP (mist.lansce.lanl.gov).
[60] B. Karvaly, I. Hevesi, *Z. Naturforsch. Teil A* **1971**, *26*, 245.
[61] Kritzner, J. Kuta, *Pure Appl. Chem.* **1984**, 56, 461.

Received: April 13, 2000 [F2421]

0947-6539/01/0703-0748 $ 17.50+.50/0